Electronic Supplementary Material (ESI) for Chemical Science.

A role of intermolecular interaction modulating thermal diffusivity in organosuperelastic and organoferroelastic cocrystals

Subham Ranjan[1], Ryota Morioka[2], Meguya Ryu[3], Junko Morikawa[2]*, and Satoshi Takamizawa[1]*

[1]Department of Materials System Science, Graduate School of Nanobioscience, Yokohama City University, 22-2 Seto, Kanazawa-ku, Yokohama, Kanagawa 236-0027, Japan

[2]School of Materials and Chemical Technology, Tokyo Institute of Technology, Tokyo 152-8550, Japan

[3] National Metrology Institute of Japan (NMIJ), National Institute of Advanced Industrial Science and Technology (AIST), Tsukuba Central 3, 1-1-1 Umezono, Tsukuba 305-8563, Japan

E-mail: morikawa.j.aa@m.titech.ac.jp ; staka@yokohama-cu.ac.jp

Table of contents: **Page**

Other supporting material

Shear stress-induced deformation behaviors under the microscope:

Movie S1. Shear stress-induced mechanical deformation on $(0\bar{1}1)$ plane of cocrystal **1** by a pair of tweezers.

Movie S2. Shear stress-induced mechanical deformation on (001) plane of cocrystal **2** by a pair of tweezers.

EXPERIMENTAL SECTION

Materials

1,4-diiodotetrafluorobenzene, 1,2-bis(4-pyridyl)ethane, and pyrene were procured from Sigma–Aldrich and were used without any additional purification.

Preparation of Single Crystals of cocrystals

For the preparation of cocrystal **1**, 1,4-diiodotetrafluorobenzene, and 1,2-bis(4-pyridyl)ethane in an equimolar ratio of 1:1 was dissolved in dichloromethane. Further, to prepare cocrystal **2**, 1,4-diiodotetrafluorobenzene and pyrene in an equimolar ratio of 1:1 was dissolved in ethanol. Slow evaporation of the respective solution yielded colorless block-shaped single crystals of cocrystals 1 and 2.

Microscopic Observation. The mechanical deformation of crystals was initially investigated by applying force with tweezers and was recorded by an optical microscope (SZ61, Olympus Co.) with inbuilt polarizing plates and a digital camera.

Force Measurements.

The shear test was carried out using a Universal testing machine at room temperature. A crystal was attached to a glass base and then the shear stress was applied on the crystal face $(0\bar{1}1)$ in cocrystal **1** and (001) in cocrystal **2** using a glass jig at a displacement rate of 3 μm sec^{-1}. The deformation behavior was observed using a polarized light microscope. The detailed calculations can be found in previous works.[1, 2]

Single-Crystal X-ray Structure Analysis. Single-crystal X-ray diffraction (SCXRD) data of the cocrystals **1** and **2** with parent (α_M) and deformed daughter (α_D) of the obtained single crystals were collected on a Bruker D8 VENTURE (PHOTON III 14) using a graphite monochromated Mo Kα radiation (λ = 0.71073 Å) at room temperature (rt). Intrinsic phasing methods (SHELXT)[3] were used to solve the structure, and full-matrix least-squares calculations on F^2 (SHELXL)[4, 5] were used to refine it. Non-hydrogen atoms were refined anisotropically, while hydrogen atoms were fixed at calculated positions using a riding model approximation. Mercury CSD was used to measure Miller plane interplanar angles.

Thermal diffusivity analysis. The directional thermal diffusivity of the single crystals **1** and **2** were measured by μ-TWA method. The single crystal having a size of approximately 100 μ

m × 100 μm × 100 μm (thickness) was inserted between an ITO micro heater (area-size: 1 mm × 250 μm) and a sputtered micro-thermocouple (TC) type sensor (area size: 20 μm × 20 μm) fabricated on borosilicate glass. The thermal contact was monitored using the originally made sample cell aligner with optics. The periodic Joule heating was applied from the heater and detected by the micro-TC heater. The detailed configuration of the measurement can be found in previous works.[6] The detected signal was analyzed based on the principle of temperature wave propagation. The thermal diffusivity was estimated from its phase delay between the heater and sensor surfaces. The phase delay of the periodic temperature response can be written as follows.

$$\Delta\theta = -\sigma + \tan^{-1}\left\{\frac{-(1-b)^2\exp(-2\sigma)\sin 2\sigma}{(1+b)^2-(1-b)^2\exp(-2\sigma)\cos 2\sigma}\right\} - \frac{\pi}{4}$$

$$\sigma = \sqrt{\frac{\pi f}{\alpha}}d$$

$$b = \frac{e_s}{e}$$

Here, α is the thermal diffusivity along the thickness direction, d is the thickness of the sample, f is the frequency of the applied temperature wave, e is the thermal effusivity of the sample, and e_s is the thermal effusivity of the substrate. At sufficiently high frequency (σ "1), the first term of the equation becomes dominant, and frequency dependency of the phase delay data can be analyzed by a linear function with the slope correlated with the thermal diffusivity along the thickness direction. The frequency of the temperature wave was typically set between 10 Hz – 1.4 kHz range under the thermally thick conditions for the measurement of frequency dependence of the phase delay.

Table S1. Crystallographic data of mother and daughter domain of cocrystals **1** and **2**.

Domain	α_M (cocrystal **1**)	α_D (cocrystal **1**)	α_M (cocrystal **2**)	α_D (cocrystal **2**)
T /K	296(2)	296(2)	296(2)	296(2)
Empirical formula	C_{18} H_{12} I_2 F_4 N_2* (Mother Domain)	C_{18} H_{12} I_2 F_4 N_2* (Daughter Domain)	C_{22} H_{10} I_2 F_4 (Mother Domain)	C_{22} H_{10} I_2 F_4 (Daughter Domain)
Crystal system	triclinic	triclinic	monoclinic	monoclinic
Space group	$P\bar{1}$	$P\bar{1}$	$P2_1/c$	$P2_1/c$
a /Å	5.03760(10)	5.03720(10)	8.3909(5)	8.3940(7)
b /Å	9.9157(3)	9.9139(3)	18.3230(11)	18.3051(13)
c /Å	10.6198(3)	10.6213(3)	13.1994(9)	13.1815(9)
α /°	64.7690(10)	64.7660(10)	90	90
β /°	82.1290(10)	82.1070(10)	105.330(2)	105.310(2)
γ /°	87.8810(10)	87.9050(10)	90	90
V /Å^3	475.21(2)	475.11(2)	1957.2(2)	1953.5(3)
Z	2	2	4	4
ρ_{calcd} [g cm^{-3}]	2.048	2.048	2.050	2.054
F(000)	276	276	1136	1136
μ [mm^{-1}]	3.35	3.351	3.255	3.261
index ranges	-5 ≤ h ≤ 5, -11 ≤ k ≤ 11, -12 ≤ l ≤ 12	-5 ≤ h ≤ 5, -11 ≤ k ≤ 11, -12 ≤ l ≤ 12	-9 ≤ h ≤ 9, -20 ≤ k ≤ 21, -15 ≤ l ≤ 15	-10 ≤ h ≤ 10, -23 ≤ k ≤ 22, -16 ≤ l ≤ 17
Refs collected	1662	1662	3443	4466
Goodness of fit	1.026	1.118	1.071	1.014
R_1(I>2σ (all data))	0.0157	0.0162	0.0359	0.0460
wR_2(I>2σ (all data))	0.0405	0.0366	0.0894	0.1117
CCDC No.	2256404	2256405	2256406	2256407

*Unique part is half composition.

Cocrystal **1** (100)

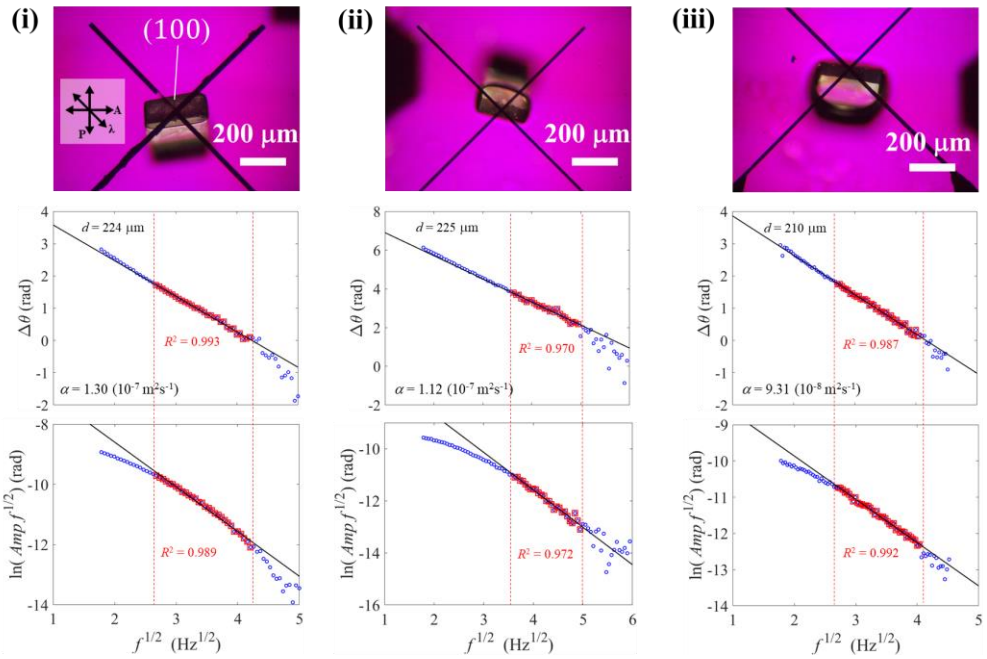

Cocrystal **1** ($0\bar{1}1$)

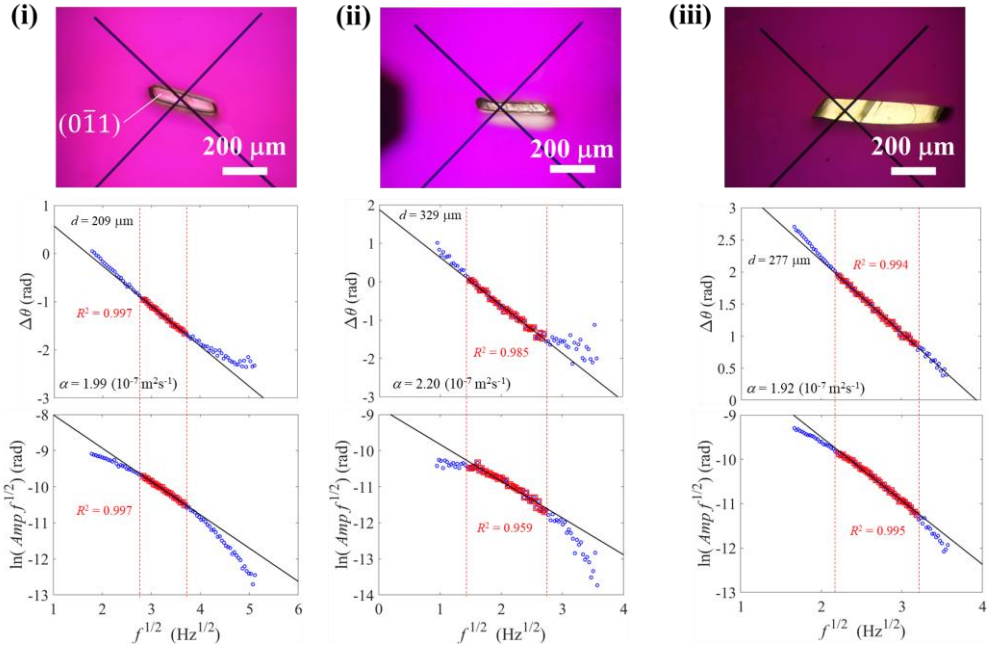

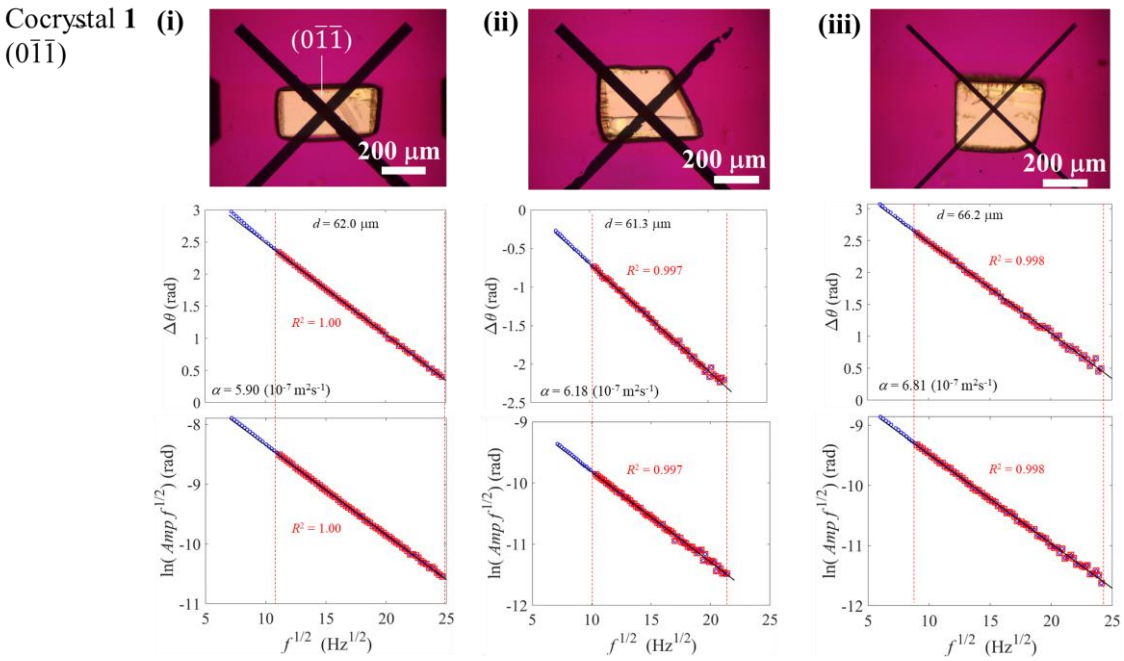

Figure S1. Frequency dependency of phase delay measured along [100], [0$\bar{1}$1], and [0$\bar{1}\bar{1}$], directions of cocrystal **1**. The measurements were conducted in triplicate, which is represented by (i), (ii), and (iii) in the individual case.

Table S2. Summary of measured thermal diffusivity of cocrystal **1** along [100], [0$\bar{1}$1], and [0$\bar{1}\bar{1}$] directions. Errors of the mean were calculated as 95% confidence intervals.

Direction	Sample	Thickness (µm)	$\alpha_{\Delta\theta}$ (10^{-7}m^{2}s^{-1})	$\alpha_{\Delta\theta\ ave}$ (10^{-7}m^{2}s^{-1})	f_{min}-f_{max} (Hz)	σ_{min}-σ_{max}	R^2 ($\alpha_{\Delta\theta}$)
[100]	1	224	1.30 ± 0.04	1.12 ± 0.17	7.18-17.7	2.95-4.64	0.993
	2	225	1.12 ± 0.08		13.2-24.5	4.33-5.90	0.970
	3	210	0.931 ± 0.035		7.39-16.3	3.32-4.92	0.987
[0$\bar{1}$1]	4	209	1.99 ± 0.05	2.04 ± 0.13	8.05-13.6	2.36-3.06	0.997
	5	329	2.20 ± 0.09		2.19-7.33	1.84-3.37	0.985
	6	277	1.92 ± 0.05		4.93-10.1	2.48-3.56	0.994
[0$\bar{1}\bar{1}$]	7	62.0	5.90 ± 0.03	6.30 ± 0.43	124-609	1.59-3.53	1.00
	8	61.3	6.18 ± 0.09		107-457	1.43-2.95	0.997
	9	66.2	6.81 ± 0.08		81.3-581	1.28-3.43	0.998

Cocrystal **2** (100)

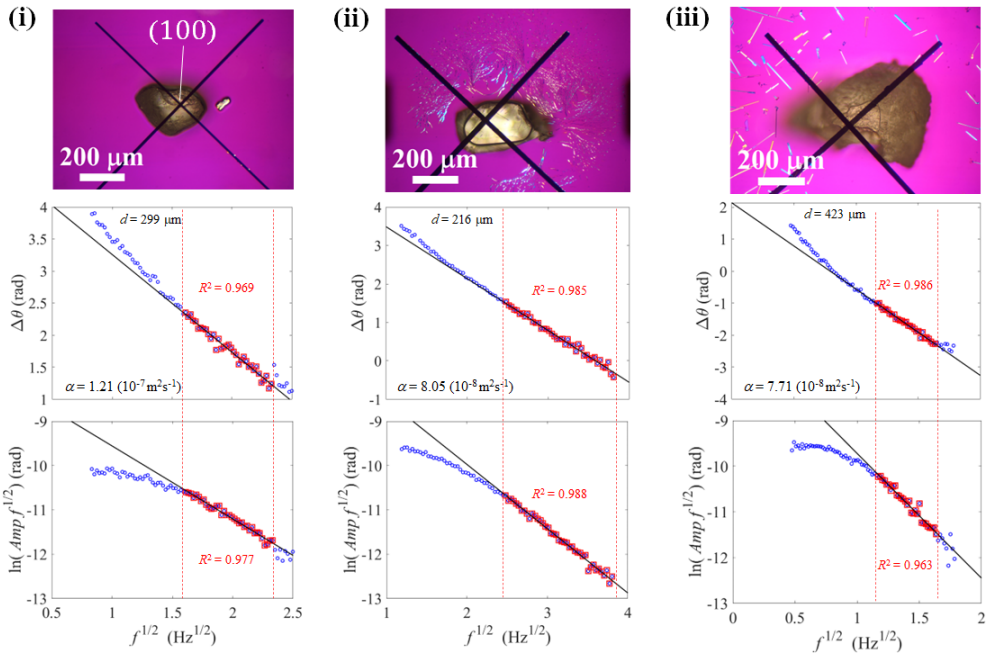

Cocrystal **2** ($0\bar{1}0$)

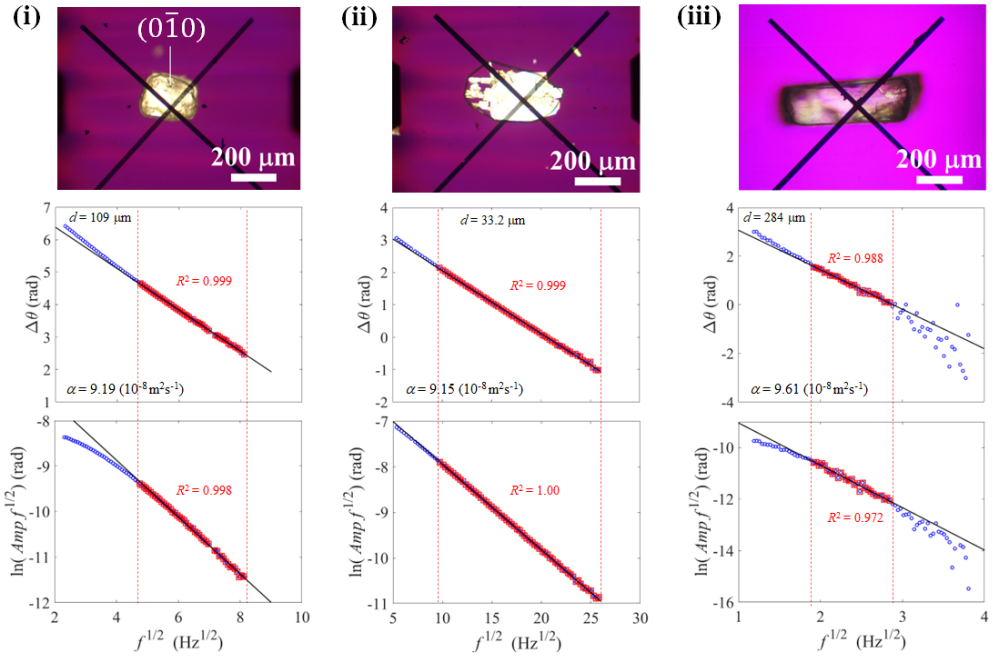

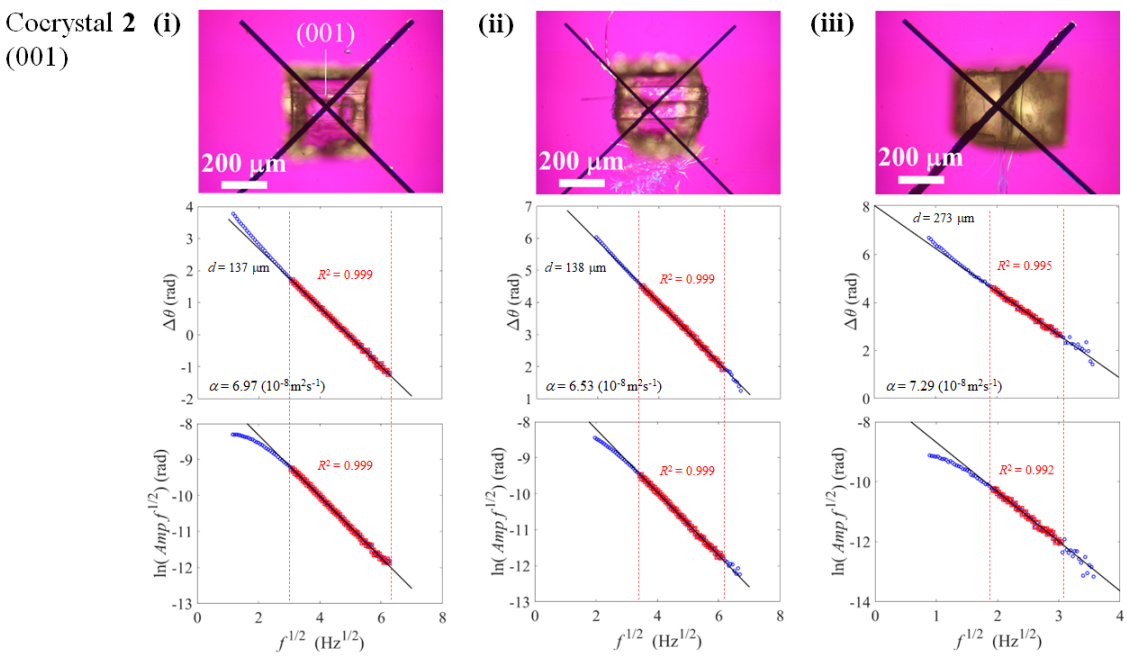

Figure S2. Frequency dependency of phase delay measured along [100], [0$\bar{1}$0], and [001] directions of cocrystal **2**. The measurements were conducted in triplicate, which is represented by (i), (ii), and (iii) in the individual case.

Table S3. Summary of measured thermal diffusivity of cocrystal **2** along [100], [0$\bar{1}$0], and [001] directions.

Direction	Sample	Thickness (μm)	$\alpha_{\Delta\theta}$ ($10^{-7}m^2s^{-1}$)	$\alpha_{\Delta\theta\ ave}$ ($10^{-7}m^2s^{-1}$)	f_{min}-f_{max} (Hz)	σ_{min}-σ_{max}	R^2 ($\alpha_{\Delta\theta}$)
[100]	10	299	1.21 ± 0.07	0.929 ± 0.226	2.60-5.42	2.46-3.55	0.969
	11	216	0.805 ± 0.032		6.16-14.5	3.35-5.13	0.985
	12	423	0.771 ± 0.036		1.37-2.67	3.16-4.41	0.986
[0$\bar{1}$0]	13	109	0.919 ± 0.007	0.932 ± 0.024	22.6-65.9	3.02-5.16	0.999
	14	33.2	0.915 ± 0.006		94.7-665	1.89-5.02	0.999
	15	284	0.961 ± 0.041		3.68-8.10	3.12-4.62	0.988
[001]	16	137	0.697 ± 0.006	0.693 ± 0.035	9.55-39.0	2.84-5.74	0.999
	17	138	0.653 ± 0.006		12.0-37.1	3.31-5.83	0.999
	18	273	0.729 ± 0.017		3.77-9.16	3.48-5.42	0.995

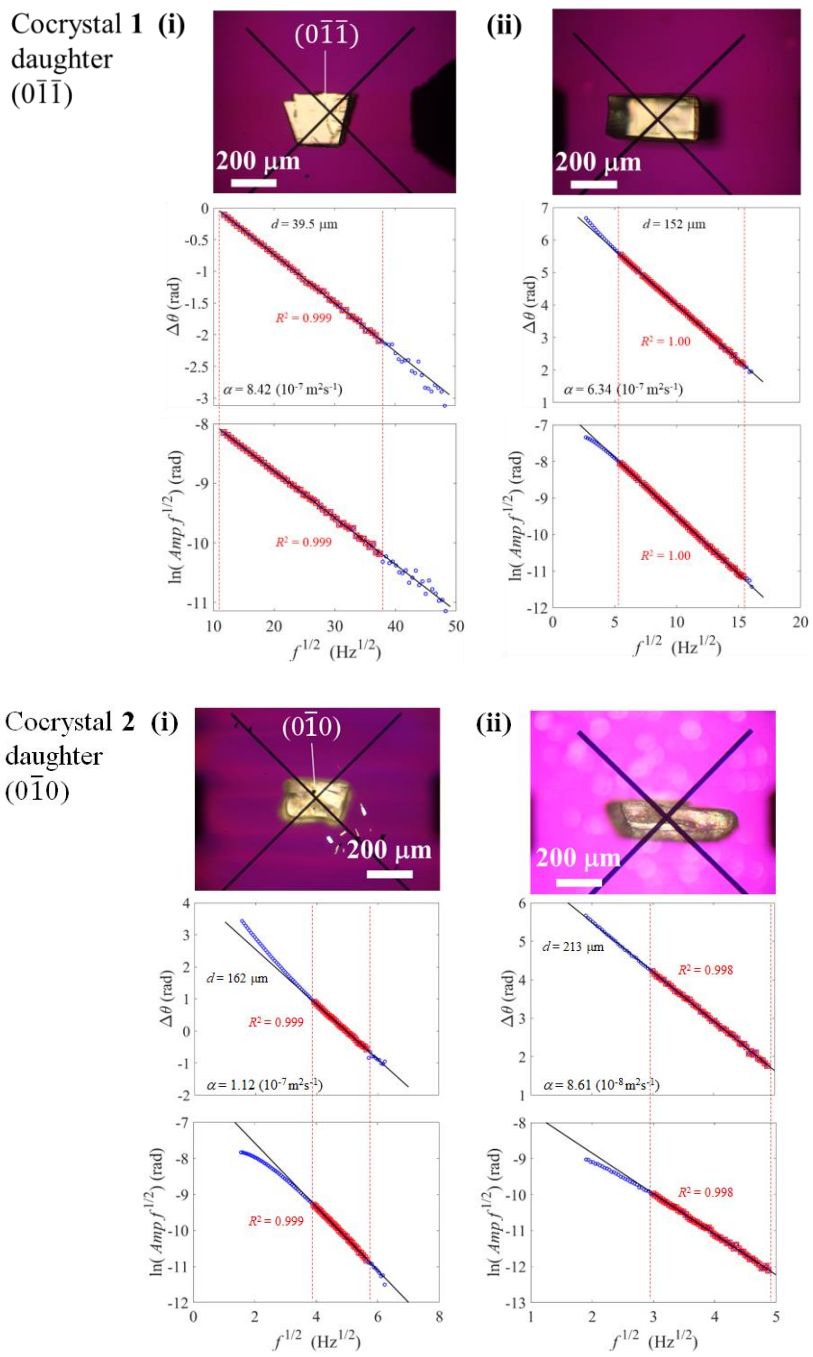

Figure S3. Frequency dependency of phase delay measured along [0$\bar{1}\bar{1}$], and [0$\bar{1}$0] directions of the daughter domain of cocrystal **1** and **2**, respectively. The measurements were conducted in duplicate, represented by (i) and (ii) in individual cases.

Table S4. Summary of measured thermal diffusivity of daughter domain of cocrystal **1** and **2** along $[0\bar{1}\bar{1}]$, and $[0\bar{1}0]$ directions, respectively.

Direction	Sample	Thickness (μm)	$\alpha_{\Delta\theta}$ ($10^{-7}m^2s^{-1}$)	$\alpha_{\Delta\theta}$ ave ($10^{-7}m^2s^{-1}$)	f_{min}-f_{max} (Hz)	σ_{min}-σ_{max}	R^2 ($\alpha_{\Delta\theta}$)
Cocrystal **1** daughter $[0\bar{1}\bar{1}]$	19	39.5	8.42 ± 0.06	7.38 ± 1.44	138-1394	0.90-2.85	0.999
	20	152	6.34 ± 0.03		29.8-235	1.85-5.19	1.00
Cocrystal **2** daughter $[0\bar{1}0]$	21	162	1.12 ± 0.01	0.991 ± 0.179	15.4-31.8	3.36-4.83	0.999
	22	213	0.861 ± 0.010		8.97-23.8	3.85-6.27	0.998

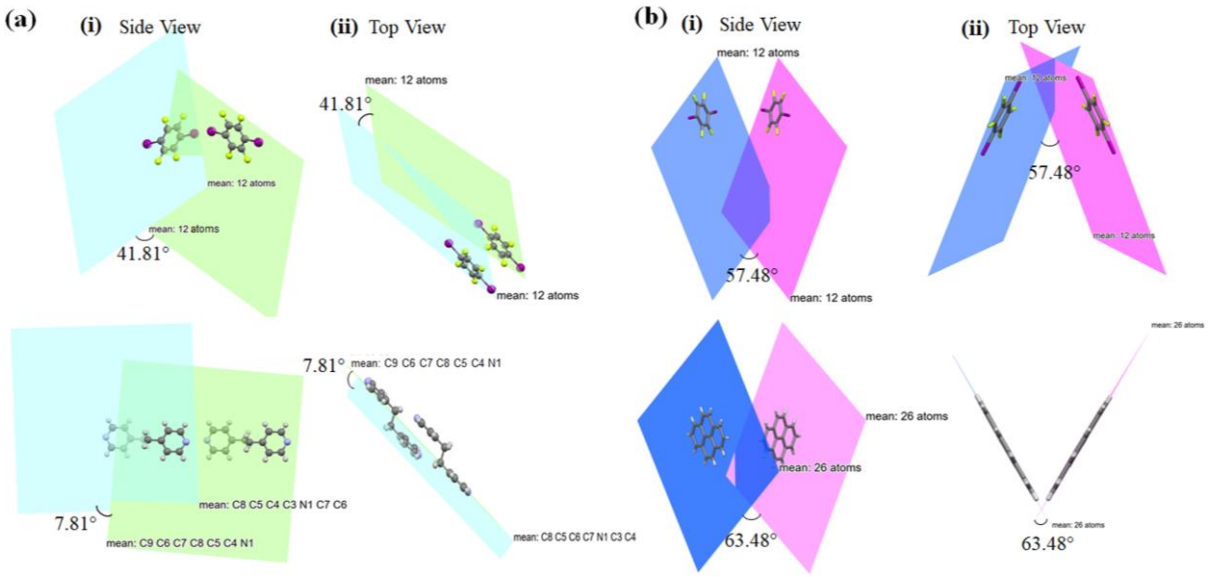

Figure S4. Estimated molecular movements (a) cocrystal **1**, (b) cocrystal **2**. Light blue and light green colored planes indicate the α_M and α_D domains of cocrystal **1**, and dark blue and light purple coloured planes indicate the α_M and α_D domains of cocrystal **2**, respectively.

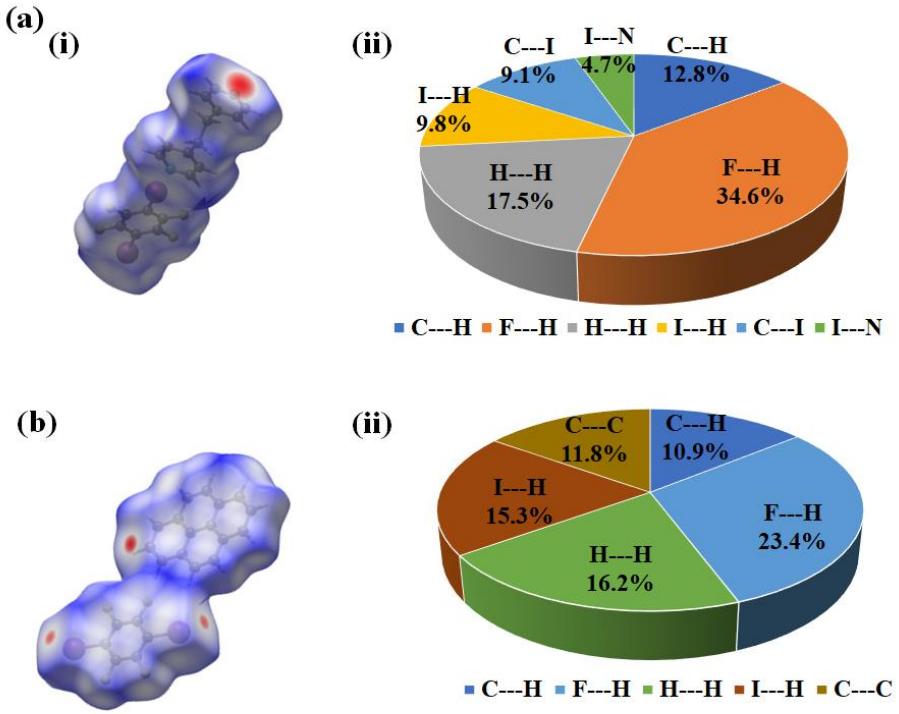

Figure S5. The relative contribution of intermolecular interactions to the Hirshfeld surface area (a & b) (i) fingerprint, and (ii) intermolecular interactions of cocrystal **1** and **2**, respectively.

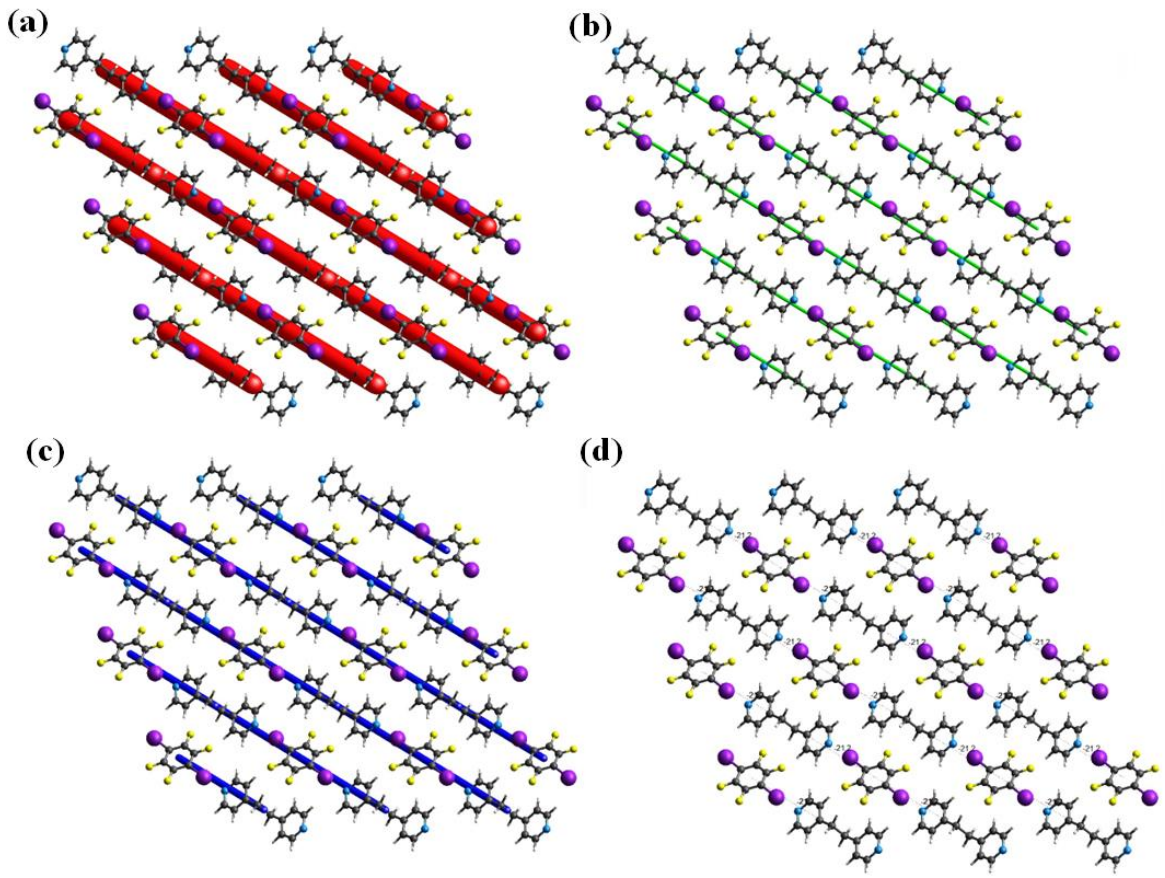

Figure S6. Energy framework along bc plane of cocrystal **1**. (a) Electrostatic, (b) dispersion, (c) total energy and (d) total interaction energy value are coloured in red, green, blue, and black, respectively. Tube size indicates the respective energy.

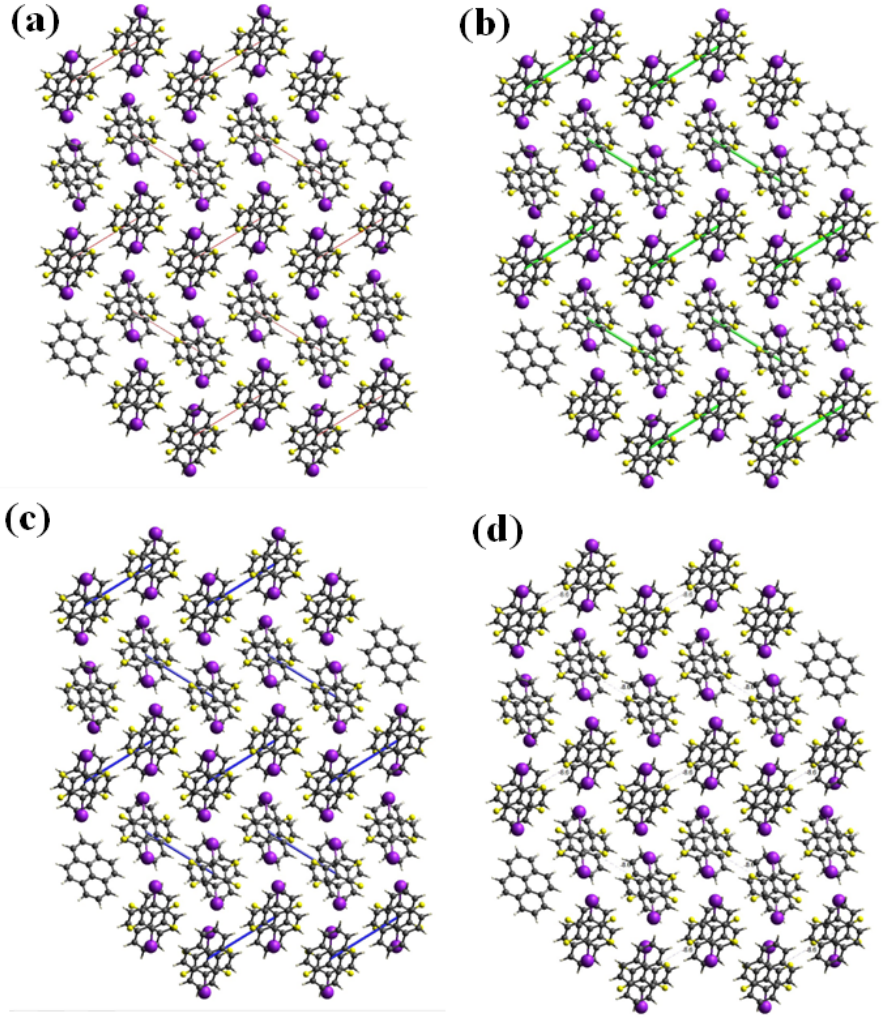

Figure S7. Energy framework along ac plane of cocrystal **2**. (a) Electrostatic, (b) dispersion, and (c) total energy and (d) total interaction energy values are coloured in red, green, blue, and black, respectively. Tube size indicates the respective energy.

References

1. S. Takamizawa and Y. Miyamoto, Superelastic organic crystals, *Angew. Chem. Int. Ed.*, 2014, **126**, 7090-7093.

2. S. H. Mir, Y. Takasaki, E. R. Engel and S. Takamizawa, Ferroelasticity in an organic crystal: a macroscopic and molecular level study, *Angew. Chem. Int. Ed.*, 2017, **56**, 15882-15885.

3. G. M. Sheldrick, SHELXT–Integrated space-group and crystal-structure determination, *Acta Crystallogr. A: Found. Adv.*, 2015, **71**, 3-8.

4. G. M. Sheldrick, A short history of SHELX, *Acta Crystallogr. A*, 2008, **64**, 112-122.

5. G. M. Sheldrick, Crystal structure refinement with SHELXL, *Acta Crystallogr. C Struct. Chem.*, 2015, **71**, 3-8.

6. M. Ryu, S. Takamizawa and J. Morikawa, Thermal diffusivity of organosuperelastic soft crystals during stress-induced phase transition, *Appl. Phys. Lett.*, 2021, **119**, 251902.

Post-acceptance modifications (Acceptance date: Oct. 15, 2023)

Page, Action, Details:

Oct. 22, 2023

Page S4, Correction, The first row equation was corrected:

Original: $\Delta\theta = -\sigma + \tan^{-1}\left\{\frac{(1-b)\exp(-2\sigma)\sin 2\sigma}{(1+b)+(1-b)\exp(-2\sigma)\cos 2\sigma}\right\}$

After modification: $\Delta\theta = -\sigma + \tan^{-1}\left\{\frac{-(1-b)^2\exp(-2\sigma)\sin 2\sigma}{(1+b)^2-(1-b)^2\exp(-2\sigma)\cos 2\sigma}\right\} - \frac{\pi}{4}$

Page S5, Addition, A footnote was added to Table S1: *Unique part is half composition.

Page S7, S9 and S11, Correction, The symbols in the first row in Tables S2-S4 were changed from *kd* to *σ*.:

Original:

Direction	Sample	Thickness (μm)	$\alpha_{\Delta\theta}$ ($10^{-7}m^2s^{-1}$)	$\alpha_{\Delta\theta\ ave}$ ($10^{-7}m^2s^{-1}$)	f_{min}-f_{max} (Hz)	kd_{min}-kd_{max}	R^2 ($\alpha_{\Delta\theta}$)

After modification:

Direction	Sample	Thickness (μm)	$\alpha_{\Delta\theta}$ ($10^{-7}m^2s^{-1}$)	$\alpha_{\Delta\theta\ ave}$ ($10^{-7}m^2s^{-1}$)	f_{min}-f_{max} (Hz)	σ_{min}-σ_{max}	R^2 ($\alpha_{\Delta\theta}$)

Page S11, Correction, The $\alpha_{\Delta\theta\ ave}$ value in the second row in Table S4 was changed from 7.40 to 7.38.

Original:

Cocrystal **1** daughter $[0\bar{1}\bar{1}]$	19	39.5	8.42 ± 0.06	7.40 ± 1.44	138-1394	0.90-2.85	0.999
	20	152	6.34 ± 0.03		29.8-235	1.85-5.19	1.00

After modification:

Cocrystal **1** daughter $[0\bar{1}\bar{1}]$	19	39.5	8.42 ± 0.06	7.38 ± 1.44	138-1394	0.90-2.85	0.999
	20	152	6.34 ± 0.03		29.8-235	1.85-5.19	1.00